MATCH
Communications in Mathematical and in Computer Chemistry

MATCH Commun. Math. Comput. Chem. **95** (2026) 405–440
ISSN: 0340–6253
doi: 10.46793/match.95-2.12025

Codimension-Two Bifurcation of a Chlorine Dioxide-Iodine-Malonic Acid Reaction System

Muhammad Asif Khan[a,*], Qamar Din[b] , Walid Abdelfattah[c]

[a]*Department of Mathematics, Faculty of Natural and Applied Sciences, The Azad Jammu and Kashmir University of Haveli, Azad Kashmir, Pakistan*

[b]*Department of Mathematics, University of Poonch Rawalakot, Azad Kashmir, Pakistan*

[c]*Department of Mathematics, College of Science, Northern Border University, Arar, Saudi Arabia*

asif31182@gmail.com, qamar.sms@gmail.com, walid.abdelfattah@nbu.edu.sa

(Received May 20, 2025)

Abstract

This work presents a comprehensive analysis of nonlinear dynamics in a discrete-time chlorine dioxide-iodine-malonic acid (CDIMA) reaction model, combining theoretical bifurcation analysis with numerical validation. Using forward Euler discretization and normal form theory, we establish the existence of codimension-two bifurcations at the system's positive fixed point, characterized by 1:2, 1:3, and 1:4 strong resonances. Numerical simulations quantitatively confirm these theoretical predictions, revealing three distinct dynamical regimes: (1) stable period-2 limit cycles emerging from 1:2

*Corresponding author.

resonance, demonstrating rhythmic bistable oscillations; (2) complex period-3 orbits arising from 1:3 resonance, indicating tripled-state nonlinear interactions; and (3) a mixed periodic-chaotic regime generated by 1:4 resonance, exhibiting sensitive dependence on initial conditions. The remarkable agreement between analytical and computational results provides robust verification of the CDIMA system's rich dynamical repertoire. These findings offer new insights into chemical oscillator control, with potential applications ranging from engineered reaction-diffusion systems to biological rhythm regulation. The integrated theoretical-numerical approach developed here establishes a general framework for investigating complex behaviors in nonlinear chemical systems.

1 Introduction

In nature, the interaction between various chemical substances often results in highly complex dynamic phenomena. The Belousov–Zhabotinsky (BZ) reaction exemplifies non-equilibrium thermodynamics, showcasing a family of reactions that produce nonlinear chemical oscillations. The oscillatory BZ reactions were first investigated by Belousov in 1958 [14] and later expanded upon by Zhabotinskii in 1964 [21]. The dynamics of chemical oscillations can exhibit significant complexity. The original BZ reaction involves over twenty reaction steps; however, many of these steps can reach equilibrium, allowing the kinetics to be simplified into three differential equations. For more detailed information on the BZ reaction, readers are directed to references [22,23]. Similarly, Lengyel et al. [1] explored another relatively simple oscillatory chemical reaction involving chlorine dioxide, iodine, and malonic acid (ClO_2–I_2–MA).

These three reactions can be outlined through the following steps

(i) The iodination of malonic acid (MA) is represented by the following reaction scheme:

$$MA + I_2 \rightarrow IMA + I^- + H^+ \tag{1}$$

(ii) The oxidation of iodide ions by chlorine dioxide radicals is described by the following reaction:

$$ClO_2 + I^- \rightarrow ClO_2^- + \frac{1}{2}I_2. \tag{2}$$

(iii) The reaction between chlorite ions and iodide ions, produced in the first two steps, to generate iodine is represented as:

$$ClO_2^- + 4I^- + 4H^+ \rightarrow Cl^- + 2I_2 + 2H_2O. \tag{3}$$

The rate equations for the chlorine dioxide-iodine-malonic acid (ClO_2–I_2–MA) reaction system are given by:

$$-\frac{d[I_2]}{dt} = \frac{c_{1a}[MA][I_2]}{c_{1b} + [I_2]}, \tag{4}$$

$$-\frac{d[ClO_2]}{dt} = c_2[ClO_2][I^-], \tag{5}$$

and

$$-\frac{d[ClO_2^-]}{dt} = c_{3a}[ClO_2^-][I^-][H^+] + c_{3b}[ClO_2^-][I^-][I_2]\frac{I^-}{u + [I^-]^2}, \tag{6}$$

where c_{1a}, c_2, c_{3a}, and c_{3b} are reaction rate constants, while c_{1b} and u describe saturation phenomena. Furthermore, the last term in Equation (6) captures the autocatalytic effect of I_2 and the self-inhibitory effect of I^- on the chlorite-iodide reaction [4]. This term is designed such that it approaches zero in two scenarios: (i) when $[I^-] \rightarrow 0$, where the reaction cannot proceed due to the absence of iodide ions, and (ii) when $[I^-] \rightarrow \infty$, where the self-inhibition effect becomes dominant. The rate equations (4-6) described above result in a five-variable model that includes the concentrations of $[ClO_2^-]$, $[I^-]$, $[ClO_2]$, $[I_2]$, and [MA]. However, the primary role of malonic acid iodination is to generate iodide ions, and ethyl acetoacetate can be used as a substitute for malonic acid (MA) [4]. Additionally, experimental observations reveal that the concentrations of iodide and chlorite ions undergo significant variations, spanning several orders of magnitude during oscillations. In contrast, the concentrations of malonic acid, chlorine dioxide, and iodine exhibit much slower changes. As a result, these concentrations can be treated as constants, allowing the system's behavior to be approximated using a two-variable model that focuses solely on the concentrations of iodide and chlorite ions. In a flow reactor

with appropriate feeding, the concentrations of chlorine dioxide, iodine, and malonic acid can be maintained nearly constant. Under these conditions, oscillations can still be observed within suitable ranges of concentrations and temperature. Therefore, we conclude that the concentrations of MA, I_2, and ClO_2 vary significantly more slowly compared to the intermediate species I^- and ClO_2^-, which undergo changes spanning several orders of magnitude during an oscillation period. By defining $X = [I^-]$, $Y = [ClO_2^-]$, and $A = [I_2]$, we derive the following equations [1]:

$$\begin{aligned} &\mathrm{A} \to \mathrm{X}; \quad r_{M1} = c_1'; \quad c_1' = c_1[\mathrm{MA}]_0, \\ &\mathrm{X} \to \mathrm{Y}; \quad r_{M2} = c_2'[\mathrm{X}]; \quad c_2' = c_2[\mathrm{ClO_2}], \\ \text{and} \quad &4\mathrm{X} + \mathrm{Y} \to \mathrm{P}; \quad r_{M3} = \frac{c_3'[\mathrm{X}][\mathrm{Y}]}{u + [\mathrm{X}]^2}; \quad c_3' = c_{3b}[\mathrm{I_2}]_0. \end{aligned}$$

Following the approach outlined in [1], we apply the transformations $X = \alpha x$, $Y = \beta y$, and $t = kt$, where $\alpha = \sqrt{u}$, $\beta = \frac{uc_2'}{c_3'}$, $k = \frac{1}{c_2'}$, $a = \frac{kc_1'}{\alpha}$, and $b = \frac{\alpha}{\beta}$. Using these transformations, we obtain the following two-dimensional system:

$$\begin{aligned} \frac{dx}{dt} &= a - x - \frac{4xy}{1 + x^2}, \\ \frac{dy}{dt} &= bx\left(1 - \frac{y}{1 + x^2}\right), \end{aligned} \tag{7}$$

where x and y represent the dimensionless concentrations of I^- and ClO_2^-, respectively, and $a > 0$, $b > 0$ are kinetic parameters. For specific values of the parameters a and b, the system (7) exhibits a stable limit cycle. For a deeper exploration of chaos and bifurcation phenomena in the BZ reaction and chemical reaction systems, see references [2, 3, 11–13]. Note that the discrete dynamical system is often more suitable than its continuous counterpart due to its rich dynamics and remarkable computational efficiency, as demonstrated in [20, 24]. Moreover, this approach proves particularly effective for nonlinear chemical oscillatory reaction models, as evidenced in [25–27]. As established by Strogatz [28], chaotic behavior can only arise in continuous systems with at least a three-dimensional phase space. Consequently, system (7) being of lower dimensionality cannot ex-

hibit chaos. In contrast, its discrete-time counterpart can manifest chaotic dynamics even in a one-dimensional mapping. To explore the chaotic behavior of system (7) in greater depth, it is suitable to examine its discrete-time counterparts. To achieve this, applying the forward Euler's scheme results in the following discrete-time version of system (7):

$$\begin{aligned} x_{n+1} &= x_n + h\left(a - x_n - \frac{4x_n y_n}{1+x_n^2}\right), \\ y_{n+1} &= y_n + bh\left(x_n - \frac{x_n y_n}{1+x_n^2}\right), \end{aligned} \tag{8}$$

where h represents the step size. In 2018, Din et al. [5] performed an in-depth analysis of the stability and Neimark-Sacker bifurcations for model (8). In 2023, Mu et al. [6] introduced a time delay into the system and analyzed the stability and chaos control of model (8). The discrete-time model of the Chlorine Dioxide-Iodine-Malonic Acid (CDIMA) reaction showcases a diverse range of nonlinear dynamical phenomena, including period-doubling bifurcations, Neimark-Sacker bifurcations, and chaotic behavior. Although research on discrete-time systems has largely concentrated on codimension-one bifurcations, exploring codimension-two bifurcations in the CDIMA reaction provides a deeper insight into the system's intricate dynamics. Fundamental aspects of bifurcation phenomena and chaotic behavior in discrete-time chemical reaction systems are thoroughly examined in [7–10, 16–19, 29–34].

The motivational aspects and the novelty of this paper are further outlined as follows:

- The CDIMA reaction is renowned for displaying a wide range of complex oscillatory patterns. Investigating how resonance phenomena, such as 1:2, 1:3, and 1:4 resonances, arise and develop within the system is essential for accurately predicting and effectively controlling the reaction's behavior.

- Resonances like 1:2, 1:3, and 1:4 play a critical role in deciphering the periodicity and synchronization of oscillatory systems. These resonances can give rise to intricate behaviors, such as quasiperiodicity and chaos, which are key to understanding how the system

transitions between stable and unstable states.

- The study reveals how 1:2, 1:3, and 1:4 resonances generate complex bifurcation structures and interactions, uncovering intricate chaotic transitions and shifts in periodicity within the system's behavior. These phenomena, previously unexplored in a discrete-time framework, provide new insights into the system's dynamics.

- The findings of the study enable the development of predictive control strategies, which can either mitigate the onset of chaos or regulate periodic behavior. By carefully tuning system parameters, it becomes possible to achieve stable oscillations or avoid chaotic regimes at specific resonance points.

The remainder of this paper is organized in the following manner:

Section 2 covers codimension-2 bifurcations, while Section 3 provides numerical simulations.

2 Codimension-two bifurcations

In this section, we examine the codimension-two bifurcation, which arises when a system undergoes qualitative changes in its dynamics as two independent parameters are varied simultaneously. Codimension-two bifurcations involve more intricate dynamics, as both parameters must be adjusted to reach the bifurcation point. This type of bifurcation often results in richer and more complex behavior, including the emergence of periodic solutions, new fixed points, and multiple oscillatory modes. In the normal form, the system incorporates two parameters, which can be understood as a control parameter and a bifurcation parameter. As the bifurcation parameters are varied, the system undergoes a sequence of transformations, including the creation and annihilation of fixed point pairs, the formation and breakdown of limit cycles, and the onset of a homoclinic bifurcation. Examples of codimension-two bifurcations encompass fold-flip bifurcations, along with 1:2, 1:3, and 1:4 strong resonances.

Chemically, these resonances correspond to distinct periodic regimes in the concentrations of key intermediates (e.g., iodine, chlorous acid) dur-

ing the CDIMA reaction. A 1:2 resonance arises when the system cycles between two well-defined chemical states, producing a stable period-2 oscillation. Likewise, 1:3 and 1:4 resonances reflect more complex periodicities, where the reaction traverses three or four successive concentration states before repeating the sequence. Such resonances represent phase-locked dynamical modes, where the system settles into a precise rhythmic pattern rather than exhibiting quasiperiodic or chaotic oscillations.

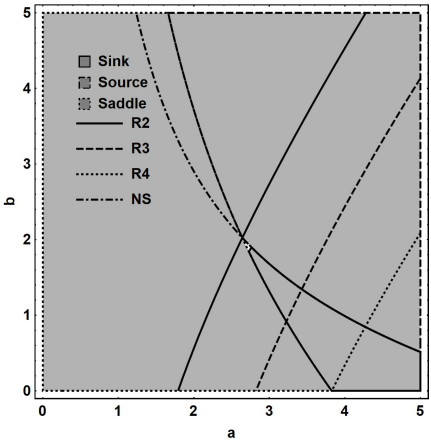

Figure 1. Topological classification for system (8).

It is easy to see that system (8) has a unique positive equilibrium point $(x_*,\ y_*) = \left(\frac{a}{5},\ \frac{a^2}{25}+1\right)$. For an in-depth examination of local stability, codimension-1 bifurcation, and chaos control of (8), refer to [5]. Specifically, we explore the existence of 1:2, 1:3, and 1:4 resonances by applying normal form theory and bifurcation theory. For this, let

$$J_{(x_*,y_*)} = \begin{pmatrix} \frac{(3a^2-125)h}{a^2+25}+1 & -\frac{20ah}{a^2+25} \\ \frac{2a^2bh}{a^2+25} & 1-\frac{5abh}{a^2+25} \end{pmatrix} \tag{9}$$

be the Jacobian matrix of system (8) evaluated at positive fixed point (x_*, y_*). Moreover, let $det(J) = \frac{a(3ah+a+5bh(5h-1))-125h+25}{a^2+25}$ and $Tr(J) = \frac{h(3a^2-5ab-125)}{a^2+25} + 2$ be the determinant and trace of $J_{(x_*,y_*)}$, respectively. Hence, the following curves determine the locations where these resonance

points occur:

$$\begin{cases} R2: \quad \mathrm{Tr}(J) = \dfrac{h\left(3a^2-5ab-125\right)}{a^2+25} + 2 = -2, \\ R3: \quad \mathrm{Tr}(J) = \dfrac{h\left(3a^2-5ab-125\right)}{a^2+25} + 2 = -1, \\ R4: \quad \mathrm{Tr}(J) = \dfrac{h\left(3a^2-5ab-125\right)}{a^2+25} + 2 = 0, \\ NS: \quad \det(J) = \dfrac{a\left(3ah+a+5bh(5h-1)\right)-125h+25}{a^2+25} = 1. \end{cases}$$

From this, it is straightforward to see that the intersections $NS \cap R_2$, $NS \cap R_3$, and $NS \cap R_4$ correspond to the 1:2, 1:3, and 1:4 resonance points, respectively. Furthermore, for $h = 0.978$, $a \in [0.001,\ 5]$, and $b \in [0.001,\ 5]$, the existence of 1:2, 1:3, and 1:4 strong resonance points in system (8) is illustrated in Fig. 1.

2.1 1:2 strong resonance

This subsection focuses on analyzing the 1:2 strong resonance for system (8) at its positive fixed point. A 1:2 strong resonance bifurcation occurs in discrete dynamical systems when two eigenvalues are -1, or equivalently the trace of the Jacobian is -2 and determinant is one. Applying this condition to Jacobian $J(x^*,\ y^*)$ of system (8), we have $T := \frac{h\left(3a^2-5ab-125\right)}{a^2+25} + 2 = -2$, and $D := \frac{a(3ah+a+5bh(5h-1))-125h+25}{a^2+25} = 1$, that is, $a = \frac{5\sqrt{(2-5h)^2}}{\sqrt{5h(3h+4)-4}}$, $b = \frac{32}{\sqrt{(2-5h)^2}\sqrt{5h(3h+4)-4}}$. For the existence of these values of a and b, we assume that $h \neq 0.4,\ 0.176607$, then positive fixed point of (8) experiences 1:2 strong resonance at $(a, b) = (a_2, b_2)$, where a_2 and b_2 are defined as follows:

$$a_2 := \frac{5\sqrt{(2-5h)^2}}{\sqrt{5h(3h+4)-4}},\ b_2 := \frac{32}{\sqrt{(2-5h)^2}\sqrt{5h(3h+4)-4}}.$$

Moreover, it is easy to see that

$$\begin{cases} (a_2, b_2) &= \left(\frac{5(2-5h)}{\sqrt{5h(3h+4)-4}}, \frac{32}{(2-5h)\sqrt{5h(3h+4)-4}} \right) \quad \text{if } h < 0.4, \\ (a_2, b_2) &= \left(\frac{5(5h-2)}{\sqrt{5h(3h+4)-4}}, \frac{32}{(5h-2)\sqrt{5h(3h+4)-4}} \right) \quad \text{if } h > 0.4. \end{cases}$$

Next, taking into account the accuracy of numerical scheme, it is more appropriate to assume that $0 < h < 0.4$, so in this case we have

$$(a_2, b_2) = \left(\frac{5(2-5h)}{\sqrt{5h(3h+4)-4}}, \frac{32}{(2-5h)\sqrt{5h(3h+4)-4}} \right).$$

Let $u_n = x_n - \frac{a}{5}$, $v_n = y_n - (\frac{a^2}{25} + 1)$, $a = a_2 + \alpha_1$ and $b = b_2 + \alpha_2$, where $\alpha = (\alpha_1, \alpha_2)$ is small perturbation parameter, then the system (8) can be transformed as follows:

$$\begin{pmatrix} u \\ v \end{pmatrix} \to (J(\alpha)) \begin{pmatrix} u \\ v \end{pmatrix} + \begin{pmatrix} f_1(u, v, \alpha) \\ f_2(u, v, \alpha) \end{pmatrix}, \tag{10}$$

where

$$\begin{aligned} J(\alpha) &:= \begin{pmatrix} h\left(3 - \frac{200}{\alpha_1^2+a_2^2+2\alpha_1 a_2+25}\right) + 1 & -\frac{20h(\alpha_1+a_2)}{\alpha_1^2+a_2^2+2\alpha_1 a_2+25} \\ \frac{2h(\alpha_1+a_2)^2(\alpha_2+b_2)}{\alpha_1^2+a_2^2+2\alpha_1 a_2+25} & 1 - \frac{5h(\alpha_1+a_2)(\alpha_2+b_2)}{\alpha_1^2+a_2^2+2\alpha_1 a_2+25} \end{pmatrix} \\ &= \begin{pmatrix} \mu_{10}(\alpha) & \mu_{01}(\alpha) \\ \nu_{10}(\alpha) & \nu_{01}(\alpha) \end{pmatrix}, \end{aligned}$$

$$\begin{cases} f_1(u, v, \alpha) = \mu_{20}(\alpha)u^2 + \mu_{11}(\alpha)uv + \mu_{02}(\alpha)v^2 + O\left((|u| + |v|)^3\right), \\ f_2(u, v, \alpha) = \nu_{20}(\alpha)u^2 + \nu_{11}(\alpha)uv + \nu_{02}(\alpha)v^2 + O\left((|u| + |v|)^3\right), \end{cases}$$

$$\begin{aligned} \mu_{20}(\alpha) &= -\frac{20h\,(\alpha_1 + a_2)\left(\alpha_1^2 + a_2^2 + 2\alpha_1 a_2 - 75\right)}{(\alpha_1^2 + a_2^2 + 2\alpha_1 a_2 + 25)^2}, \\ \mu_{11}(\alpha) &= \frac{100h\,(\alpha_1 + a_2 - 5)\,(\alpha_1 + a_2 + 5)}{(\alpha_1^2 + a_2^2 + 2\alpha_1 a_2 + 25)^2}, \ \mu_{02}(\alpha) = 0, \end{aligned}$$

$$\nu_{20}(\alpha) = -\frac{5h\,(\alpha_1+a_2)\left(\alpha_1^2+a_2^2+2\alpha_1a_2-75\right)(\alpha_2+b_2)}{\left(\alpha_1^2+a_2^2+2\alpha_1a_2+25\right)^2},$$
$$\nu_{11}(\alpha) = \frac{25h\,(\alpha_1+a_2-5)\,(\alpha_1+a_2+5)\,(\alpha_2+b_2)}{\left(\alpha_1^2+a_2^2+2\alpha_1a_2+25\right)^2},\ \nu_{02}(\alpha)=0.$$

Next, at $\alpha_1=\alpha_2=0$, we take $\alpha=(0,0)=O$, and $J(O)$ is given as follows:

$$J(O) := \begin{pmatrix} \frac{4}{5h}-3 & \frac{(5h-2)\sqrt{5h(3h+4)-4}}{10h} \\ \frac{16-40h}{5h\sqrt{5h(3h+4)-4}} & 1-\frac{4}{5h} \end{pmatrix}. \tag{11}$$

Moreover, eigenvector of $J(O)$ associated with eigenvalue -1 is $q_0 = \begin{pmatrix} \frac{1}{4}\sqrt{5h(3h+4)-4} \\ 1 \end{pmatrix}$ and its generalized eigenvector associated with eigenvalue -1 is $q_1 = \begin{pmatrix} \frac{5h\sqrt{5h(3h+4)-4}}{8(2-5h)} \\ 0 \end{pmatrix}$. In addition, the eigenvector and generalized eigenvector of $J(O)^T$ associated with eigenvalues -1, respectively are $p_0 = \begin{pmatrix} 1 \\ 0 \end{pmatrix}$ and $p_1 = \begin{pmatrix} -\frac{4(10h-4)}{5h\sqrt{5h(3h+4)-4}} \\ \frac{10h-4}{5h} \end{pmatrix}$, where q_0, q_1, p_0, p_1 satisfy the following conditions:

$$\begin{cases} J(O)q_0 = -q_0, \\ J(O)q_1 = -q_1 + q_0, \\ J(O)^T p_0 = -p_0, \\ J(O)^T p_1 = -p_1 + p_0, \\ \langle p_0, q_0\rangle = \langle p_1, q_1\rangle = 1, \\ \langle p_0, q_1\rangle = \langle p_1, q_0\rangle = 0. \end{cases}$$

Taking into account the aforementioned relations, we consider the following transformation:

$$\begin{pmatrix} u \\ v \end{pmatrix} = \begin{pmatrix} \frac{1}{4}\sqrt{5h(3h+4)-4} & \frac{5h\sqrt{5h(3h+4)-4}}{8(2-5h)} \\ 1 & 0 \end{pmatrix} \begin{pmatrix} w \\ z \end{pmatrix}. \tag{12}$$

From (10) and (12), it follows that:

$$\begin{pmatrix} w \\ z \end{pmatrix} \to \begin{pmatrix} p_{10}(\alpha) - 1 & 1 + p_{01}(\alpha) \\ q_{10}(\alpha) & q_{01}(\alpha) - 1 \end{pmatrix} \begin{pmatrix} w \\ z \end{pmatrix} + \begin{pmatrix} f_3(w, z, \alpha) \\ f_4(w, z, \alpha) \end{pmatrix}. \tag{13}$$

where

$$p_{10}(\alpha) = \frac{1}{4}\sqrt{5h(3h+4) - 4}\nu_{10}(\alpha) + \nu_{01}(\alpha) + 1,$$

$$p_{01}(\alpha) = \frac{5h\sqrt{5h(3h+4) - 4}\nu_{10}(\alpha)}{8(2 - 5h)} - 1,$$

$$q_{10}(\alpha) = \frac{(5h-2)((5h(3h+4) - 4)\nu_{10}(\alpha) - 16\mu_{01}(\alpha))}{10h\sqrt{5h(3h+4) - 4}} + \frac{2(5h-2)(\nu_{01}(\alpha) - \mu_{10}(\alpha))}{5h},$$

$$q_{01}(\alpha) = -\frac{1}{4}\sqrt{5h(3h+4) - 4}\nu_{10}(\alpha) + \mu_{10}(\alpha) + 1,$$

$$f_3(w, z, \alpha) = f_2\left(\frac{\sqrt{5h(3h+4) - 4}(2(5h-2)w - 5hz)}{8(5h-2)}, w, \alpha\right),$$

$$f_4(w, z, \alpha) = \frac{(8(2-5h))f_1\left(\frac{\sqrt{5h(3h+4)-4}(2(5h-2)w-5hz)}{8(5h-2)}, w, \alpha\right)}{5h\sqrt{5h(3h+4) - 4}} + 2f_2\left(\frac{\sqrt{5h(3h+4) - 4}(2(5h-2)w - 5hz)}{8(5h-2)}, w, \alpha\right) - \left(\frac{4}{5h}\right) f_2\left(\frac{\sqrt{5h(3h+4) - 4}(2(5h-2)w - 5hz)}{8(5h-2)}, w, \alpha\right).$$

Next, we assume the following invertible linear transformation:

$$\begin{pmatrix} w \\ z \end{pmatrix} = M \begin{pmatrix} \bar{w} \\ \bar{z} \end{pmatrix}, \tag{14}$$

where

$$M = \begin{pmatrix} 1 + p_{01}(\alpha) & 0 \\ -p_{01}(\alpha) & 1 \end{pmatrix}.$$

From (13) and (15), it follows that:

$$\begin{pmatrix} \bar{w} \\ \bar{z} \end{pmatrix} \to \begin{pmatrix} -1 & 1 \\ \omega_1(\alpha) & \omega_2(\alpha) - 1 \end{pmatrix} \begin{pmatrix} \bar{w} \\ \bar{z} \end{pmatrix} + \begin{pmatrix} f_5(\bar{w}, \bar{z}, \alpha) \\ f_6(\bar{w}, \bar{z}, \alpha) \end{pmatrix}, \quad (15)$$

where

$$\begin{aligned} \omega_1(\alpha) &= q_{10}(\alpha) + p_{01}(\alpha)q_{10}(\alpha) - p_{10}(\alpha)q_{01}(\alpha), \\ \omega_2(\alpha) &= p_{10}(\alpha) + q_{01}(\alpha), \\ f_5(\bar{w}, \bar{z}, \alpha) &= \left(\frac{1}{1 + p_{01}(\alpha)} \right) f_3 \left(\bar{w}(1 + p_{01}(\alpha)), \bar{z} - \bar{w}p_{10}(\alpha), \alpha \right), \\ f_6(\bar{w}, \bar{z}, \alpha) &= \left(\frac{p_{10}(\alpha)}{1 + p_{01}(\alpha)} \right) f_3 \left(\bar{w}(1 + p_{01}(\alpha)), \bar{z} - \bar{w}p_{10}(\alpha), \alpha \right) \\ &\quad + f_4 \left(\bar{w}(1 + p_{01}(\alpha)), \bar{z} - \bar{w}p_{10}(\alpha), \alpha \right). \end{aligned}$$

Taking into account $\omega_1(\alpha)$ and $\omega_2(\alpha)$, we define the following matrix at $\alpha = (0, 0) = O$:

$$\begin{aligned} \zeta(O) &= \begin{pmatrix} \frac{\partial \omega_1}{\partial \alpha_1}(0,0) & \frac{\partial \omega_1}{\partial \alpha_2}(0,0) \\ \frac{\partial \omega_2}{\partial \alpha_1}(0,0) & \frac{\partial \omega_2}{\partial \alpha_2}(0,0) \end{pmatrix} \\ &= \begin{pmatrix} \frac{\sqrt{5h(3h+4)-4}(3h(5h+4)-4)}{50h^2} & \frac{(2-5h)^2\sqrt{5h(3h+4)-4}}{40h} \\ -\frac{(3h-2)\sqrt{5h(3h+4)-4}(5h(5h+6)-8)}{100h^2(5h-2)} & \frac{(5h-2)\sqrt{5h(3h+4)-4}}{40h} \end{pmatrix}. \end{aligned}$$

Then by simple calculation $\det \zeta(O)$ is obtained as follows:

$$\det \zeta(O) = \frac{(5h(h(15h + 14) - 12) + 8)^2}{4000h^3}. \quad (16)$$

Condition (16) is called transversality condition and it is supposed to be true. Next, we apply $\omega_1(\alpha_1, \alpha_2)$ and $\omega_2(\alpha_1, \alpha_2)$ for the following parametri-

zation in the neighborhood of $\alpha_1 = 0$ and $\alpha_2 = 0$:

$$\gamma_1 = \omega_1(\alpha_1, \alpha_2), \quad \gamma_2 = \omega_2(\alpha_1, \alpha_2).$$

Then, α_1 and α_2 can be expressed in terms of γ_1 and γ_2 as follows:

$$\begin{cases} \alpha_1 = \dfrac{100h^2\left(\gamma_1 + \gamma_2(2-5h)\right)}{(5h-2)(5h(3h+4)-4)^{3/2}}, \\ \alpha_2 = \dfrac{40h}{(5h-2)^3\left(5h(3h+4)-4\right)^{3/2}}\Big[\gamma_1\left(3h-2\right)\left(5h(5h+6)-8\right) \\ \qquad\qquad + 2\gamma_2\left(h\left(15h(5h+2)-44\right)+8\right)\Big]. \end{cases} \tag{17}$$

Using (17) in (15), we have the following mapping:

$$\begin{pmatrix} \bar{w} \\ \bar{z} \end{pmatrix} \to \begin{pmatrix} -1 & 1 \\ \gamma_1 & -1+\gamma_2 \end{pmatrix} \begin{pmatrix} \bar{w} \\ \bar{z} \end{pmatrix} + \begin{pmatrix} f_7(\bar{w}, \bar{z}, \gamma) \\ f_8(\bar{w}, \bar{z}, \gamma) \end{pmatrix}, \tag{18}$$

where

$$\begin{cases} f_7(\bar{w}, \bar{z}, \gamma) = g_{20}(\gamma)\bar{w}^2 + g_{11}(\gamma)\bar{w}\bar{z} + g_{02}(\gamma)\bar{z}^2, \\ f_8(\bar{w}, \bar{z}, \gamma) = h_{20}(\gamma)\bar{w}^2 + h_{11}(\gamma)\bar{w}\bar{z} + h_{02}(\gamma)\bar{z}^2, \end{cases}$$

$\gamma = (\gamma_1, \gamma_2)$ and at $(\gamma_1, \gamma_2) = (0, 0) = O$, one may compute easily

$$\begin{aligned} g_{20}(O) &= \frac{(5h(3h+4)-4)(h(5h+16)-4)}{40h^2(5h-2)}, \\ g_{11}(O) &= -\frac{(5h(3h+4)-4)(5h(h(5h+17)-8)+4)}{40(2-5h)^2h^2}, \\ g_{02}(O) &= \frac{(5h(h+4)-4)(5h(3h+4)-4)}{32(2-5h)^2h}, \\ h_{20}(O) &= \frac{(5h(3h+4)-4)(h(5h+16)-4)}{40h^2}, \\ h_{11}(O) &= -\frac{(5h(3h+4)-4)(5h(h(5h+17)-8)+4)}{40h^2(5h-2)}, \\ h_{02}(O) &= \frac{(5h(h+4)-4)(5h(3h+4)-4)}{32h(5h-2)}. \end{aligned}$$

Then according to Lemma 9.9 [[15], p. 437], there exists a near–identity

map such that system (15) can be transformed as follows:

$$\begin{pmatrix} z_1 \\ z_2 \end{pmatrix} \to \begin{pmatrix} -1 & 1 \\ \gamma_1 & -1+\gamma_2 \end{pmatrix} \begin{pmatrix} z_1 \\ z_2 \end{pmatrix} + \begin{pmatrix} 0 \\ A(\gamma_1,\gamma_2)z_1^3 + B(\gamma_1,\gamma_2)z_1^2 z_2 \end{pmatrix} + O(|z_1+z_2|^4), \tag{19}$$

where

$$\begin{cases} A(\gamma) = g_{20}(\gamma)h_{20}(\gamma) + \dfrac{1}{2}h_{20}^2(\gamma) + \dfrac{1}{2}h_{20}(\gamma)h_{11}(\gamma), \\ B(\gamma) = \dfrac{1}{2}g_{20}(\gamma)h_{11}(\gamma) + \dfrac{5}{4}h_{20}(\gamma)h_{11}(\gamma) + h_{20}^2(\gamma) \\ \qquad + h_{20}(\gamma)h_{02}(\gamma) + \dfrac{1}{2}h_{11}^2(\gamma) + 3g_{20}^2(\gamma) \\ \qquad + \dfrac{5}{2}g_{20}(\gamma)h_{20}(\gamma) + \dfrac{5}{2}g_{11}(\gamma)h_{20}(\gamma). \end{cases}$$

Moreover, taking into account simplicity and further requirement, we compute $A(\gamma)$ and $B(\gamma)$ at $(\gamma_1,\gamma_2) = (0,0) = O$ as follows:

$$A(O) = -\frac{(5(h-4)h+4)(4-5h(3h+4))^2(h(5h+16)-4)}{3200h^4(5h-2)},$$

and

$$B(O) = \frac{3}{25h^4} - \frac{207}{100h^3} + \frac{1531h^2}{32} + \frac{297}{25h^2} + \frac{13339h}{320} - \frac{1641}{80h} + \frac{225h^4}{128} + + \frac{4125h^3}{256} + \frac{192}{25(5h-2)} + \frac{128}{25(5h-2)^2} - \frac{7391}{400}.$$

Taking into account theoretical results cited in [15] and the above computations, we have the following result.

Theorem 1. *Consider system* (19) *with parameters set as* $(a,b) = (a_2,b_2)$ *and* $0.176607 < h < 0.4$. *Assume the non-degeneracy condition holds true:*

$$A(O)\,(B(O) + 3A(O)) \neq 0.$$

Then, in the (γ_1,γ_2)*-parameter plane, the system exhibits the following local bifurcations:*

(i) The trivial fixed point $(0,0)$ *undergoes a non-degenerate period-doubling bifurcation on the curve given by*

$$\left\{(\gamma_1,\gamma_2)\in\mathbb{R}^2:\gamma_1=0,\ \gamma_2\neq 0\right\}.$$

(ii) The trivial fixed point $(0,0)$ *undergoes a non-degenerate Neimark-Sacker bifurcation on the curve*

$$\left\{(\gamma_1,\gamma_2)\in\mathbb{R}^2:\gamma_1+\gamma_2=0,\ \gamma_1\neq 0\right\}.$$

This bifurcation is supercritical if $B(O)+3A(O)>0$.

(iii) Provided that $A(O)<0$*, the 2-cycle that emerges from the period-doubling bifurcation undergoes a non-degenerate Neimark-Sacker bifurcation. This occurs on the curve defined by*

$$\left\{(\gamma_1,\gamma_2)\in\mathbb{R}^2:\gamma_2=\left(2+\frac{B(O)}{A(O)}\right)\gamma_1+O\left(\gamma_1^2\right),\ \gamma_1>0\right\}.$$

This bifurcation of the 2-cycle is supercritical if $B(O)+3A(O)<0$.

2.2 1:3 strong resonance

In discrete dynamical systems, a 1:3 resonance bifurcation occurs when the Jacobian matrix at a fixed point possesses two eigenvalues, specifically $-\frac{1}{2}\pm\iota\frac{\sqrt{3}}{2}$, lying on the unit circle, and no additional eigenvalues are present on the unit circle.

If a and b are taken as bifurcation parameters, the characteristic equation of the variational matrix for system (8) evaluated at the point (x_*,y_*) will have eigenvalues $-\frac{1}{2}\pm\iota\frac{\sqrt{3}}{2}$ under the condition that the following requirement is met:

$$\begin{cases}2+\dfrac{h\left(3a^2-5ab-125\right)}{a^2+25}=-1,\\[2ex]\dfrac{a(3ah+a+5bh(5h-1))-125h+25}{a^2+25}=1.\end{cases}\tag{20}$$

Next, assume that $h \neq 0.17082$, then we have the following solution of system (20) for a and b:

$$\begin{cases} a_3 := \dfrac{5\sqrt{5h(5h-3)+3}}{\sqrt{15h(h+1)-3}}, \\ b_3 := \dfrac{8\sqrt{3}}{\sqrt{5h(h+1)-1}\sqrt{5h(5h-3)+3}}. \end{cases} \tag{21}$$

Next, assuming $u_n = x_n - x_*$, $v_n = y_n - y_*$ and $a = a_3 + \beta_1$, $b = b_3 + \beta_2$, where β_1 and β_2 are small perturbation parameters. Under these assumptions, (8) transforms into the following map:

$$\begin{pmatrix} u \\ v \end{pmatrix} \to \begin{pmatrix} \sigma_{10}(\beta) & \sigma_{01}(\beta) \\ \tau_{10}(\beta) & \tau_{01}(\beta) \end{pmatrix} \begin{pmatrix} u \\ v \end{pmatrix} + \begin{pmatrix} g_1(u,v,\beta) \\ g_2(u,v,\beta) \end{pmatrix}, \tag{22}$$

where $\beta = (\beta_1, \beta_2)$

$$\begin{cases} \sigma_{10}(\beta) = h\left(3 - \dfrac{200}{a_3^2 + 2a_3\beta_1 + \beta_1^2 + 25}\right) + 1, \\ \sigma_{01}(\beta) = -\dfrac{20h\,(a_3+\beta_1)}{a_3^2 + 2a_3\beta_1 + \beta_1^2 + 25}, \\ \tau_{10}(\beta) = \dfrac{2h\,(a_3+\beta_1)^2\,(\beta_2+b_3)}{a_3^2 + 2a_3\beta_1 + \beta_1^2 + 25}, \\ \tau_{01}(\beta) = 1 - \dfrac{5h\,(a_3+\beta_1)(\beta_2+b_3)}{a_3^2 + 2a_3\beta_1 + \beta_1^2 + 25}. \end{cases}$$

$$\begin{cases} g_1(u,v,\beta) = \sigma_{20}(\beta)u^2 + \sigma_{11}(\beta)uv + O\left((|u|+|v|)^3\right), \\ g_2(u,v,\beta) = \tau_{20}(\beta)u^2 + \tau_{11}(\beta)uv + O\left((|u|+|v|)^3\right), \end{cases}$$

$$\sigma_{20}(\beta) = -\frac{20h\,(a_3+\beta_1)\left(a_3^2 + 2a_3\beta_1 + \beta_1^2 - 75\right)}{\left(a_3^2 + 2a_3\beta_1 + \beta_1^2 + 25\right)^2},$$

$$\sigma_{11}(\beta) = \frac{100h\,(a_3+\beta_1-5)\,(a_3+\beta_1+5)}{\left(a_3^2 + 2a_3\beta_1 + \beta_1^2 + 25\right)^2},$$

$$\tau_{20}(\beta) = -\frac{5h\,(a_3+\beta_1)\left(a_3^2 + 2a_3\beta_1 + \beta_1^2 - 75\right)(\beta_2+b_3)}{\left(a_3^2 + 2a_3\beta_1 + \beta_1^2 + 25\right)^2},$$

$$\tau_{11}(\beta) = \frac{25h\,(a_3+\beta_1-5)\,(a_3+\beta_1+5)\,(\beta_2+b_3)}{(a_3^2+2a_3\beta_1+\beta_1^2+25)^{\,2}}.$$

The characteristic equation of the Jacobian matrix $\begin{pmatrix} \sigma_{10}(\beta) & \sigma_{01}(\beta) \\ \tau_{10}(\beta) & \tau_{01}(\beta) \end{pmatrix}$ for system (22) at $\beta_1 = \beta_2 = 0$ yields eigenvalues of the form $\frac{-1}{2} \pm \frac{\sqrt{3}}{2}\iota$. Let q and p represent the eigenvectors corresponding to the Jacobian matrix of (22) and its transpose at $\beta_1 = \beta_2 = 0$, respectively, with the condition that their inner product satisfies $\langle p, q\rangle = 1$. Through direct calculation, we derive the following:

$$q = \begin{pmatrix} -15h + 6 + 5i\sqrt{3}h \\ 4\rho \end{pmatrix},$$

and

$$p = \begin{pmatrix} \frac{i}{10\sqrt{3}h} \\ \frac{5\sqrt{3}h+3i(5h-2)}{40\sqrt{3}h\rho} \end{pmatrix},$$

where

$$\rho := \sqrt{\frac{15h(5h-3)+9}{5h(h+1)-1}}.$$

Then, every $Y \in \mathbb{R}^2$ can be expressed uniquely in the following manner:

$$Y = zq + \bar{z}\bar{q}, \quad z \in \mathbb{C}.$$

Thus, the complex representation of the map (22) can be expressed as follows:

$$z \longrightarrow \left(\frac{-1}{2} + \frac{\sqrt{3}}{2}\iota\right) z + \sum_{2\le j+k\le 3} \frac{1}{j!k!} G_{jk}(\beta) z^j \bar{z}^k, \tag{23}$$

where

$$G_{20}(\beta) = -\frac{25\sqrt{3}\left(\sqrt{3}+3i\right)h^2\tau_{20}(\beta)}{\rho} - \frac{2i\left(4\sqrt{3}\rho^2\sigma_{11}(\beta) + 6\sqrt{3}\rho\sigma_{20}(\beta) - 6\sqrt{3}\rho\tau_{11}(\beta) - 9\sqrt{3}\tau_{20}(\beta)\right)}{5h\rho}$$

$$+\frac{12i\rho^2\sigma_{11}(\beta)+4\sqrt{3}\rho^2\sigma_{11}(\beta)+36i\rho\sigma_{20}(\beta)}{\sqrt{3}\rho}$$
$$+\frac{12\sqrt{3}\rho\sigma_{20}(\beta)-36i\rho\tau_{11}(\beta)-81i\tau_{20}(\beta)-9\sqrt{3}\tau_{20}(\beta)}{\sqrt{3}\rho}$$
$$+\frac{5h}{\sqrt{3}}\Big((-6i-6\sqrt{3})\,\sigma_{20}(\beta)+12i\,\tau_{11}(\beta)\Big)$$
$$+\frac{5h}{\sqrt{3}\rho}\Big((45i+9\sqrt{3})\,\tau_{20}(\beta)\Big),$$

$$G_{11}(\beta)=\frac{4i\sqrt{3}((5h-2)\rho\sigma_{11}(\beta)+(5(3-5h)h-3)\sigma_{20}(\beta))}{5h}$$
$$+\frac{\sqrt{3}\left(5(\sqrt{3}-3i)h+6i\right)}{5h\rho}\left(5h(5h-3)+3\right)\tau_{20}(\beta)$$
$$+\frac{\sqrt{3}\left(5(\sqrt{3}-3i)h+6i\right)}{5h}\,(2-5h)\,\tau_{11}(\beta),$$

$$G_{02}(\beta)=\frac{5(\sqrt{3}-3i)h+6i}{5\sqrt{3}h}\,\big(-4\rho\,\sigma_{11}(\beta)\big)$$
$$+\frac{5(\sqrt{3}-3i)h+6i}{5\sqrt{3}h}\,\big(-6+5(3+i\sqrt{3})h\big)\,\big(\sigma_{20}(\beta)-\tau_{11}(\beta)\big)$$
$$+\frac{3\left(5h(5h-3)\left(10h+3i\sqrt{3}-3\right)+6i\sqrt{3}\right)\tau_{20}(\beta)}{5h\rho},$$

and $G_{30}(\beta)=G_{21}(\beta)=G_{12}(\beta)=G_{03}(\beta)=0$.

Next, as outlined in Lemma 9.12 [[15], p. 448], a smoothly parameter-dependent change of variables exists, which enables the transformation of the map (23) into the following form:

$$w\longrightarrow\left(-\frac{1}{2}+i\frac{\sqrt{3}}{2}\right)w+P(\beta)\bar{w}^2+Q(\beta)w|w|^2+O\left(|w|^4\right),\qquad(24)$$

where at $\beta_1=\beta_2=0$, that is, $\beta=(0,0)=O$

$$P(O)=\frac{1}{2}G_{02}(O),$$

and

$$Q(O) = \left(\frac{1}{2} + \frac{i}{\sqrt{3}}\right) G_{20}(O)G_{11}(O) + \left(\frac{1}{2} - \frac{1}{2\sqrt{3}}i\right) |G_{11}(O)|^2 .$$

Following the reasoning in Lemma 9.13 ([15], p. 450), we obtain the following result.

Theorem 2. *If the parameters are set to their critical values $a = a_3$ and $b = b_3$, the system* (8) *experiences a 1:3 strong resonance at its positive fixed point. Assuming the non-degeneracy conditions $P(O) \neq 0$ and $Re(Q(O)) \neq 0$ for the normal form coefficients of map* (24) *are satisfied, the system exhibits the following dynamical behaviors in a neighborhood of the bifurcation:*

(i) The system undergoes a Neimark-Sacker bifurcation, from which a unique closed invariant curve emerges. The stability of this curve is determined by the sign of the real part of the normal form coefficient $Q(O)$. If $Re(Q(O)) < 0$, the bifurcation is supercritical, and the invariant curve is stable (attracting). Conversely, if $Re(Q(O)) > 0$, the bifurcation is subcritical, and the invariant curve is unstable (repelling).

(ii) In the vicinity of the fixed point, a pair of period-three orbits is created. One of these orbits is a saddle cycle, while the stability of the second period-three orbit is dependent on the system parameters.

(iii) The stable and unstable manifolds of the period-three saddle cycle may intersect transversally. This intersection gives rise to a homoclinic structure, which can lead to complex dynamics and chaotic behavior within specific parameter regions.

2.3 1:4 resonance

In discrete dynamical systems, a 1:4 resonance bifurcation occurs when the Jacobian matrix at a fixed point possesses two eigenvalues, specifically $\pm i$, lying on the unit circle, and no additional eigenvalues are present on the unit circle.

If a and b are taken as bifurcation parameters, the characteristic equation of the variational matrix for system (8) evaluated at the point (x_*, y_*) will have eigenvalues $\pm i$ under the condition that the following requirement is met:

$$\begin{cases} 2 + \dfrac{h\left(3a^2 - 5ab - 125\right)}{a^2 + 25} = 0, \\ \dfrac{a(3ah + a + 5bh(5h - 1)) - 125h + 25}{a^2 + 25} = 1. \end{cases} \tag{25}$$

Next, assume that $h \neq 0.16108$, then we have the following solution of system (25) for a and b:

$$\begin{cases} a_4 := \dfrac{5\sqrt{5h(5h-2)+2}}{\sqrt{5h(3h+2)-2}}, \\ b_4 := \dfrac{16}{\sqrt{5h(3h+2)-2}\sqrt{5h(5h-2)+2}}. \end{cases} \tag{26}$$

Next, assuming $u_n = x_n - x_*$, $v_n = y_n - y_*$ and $a = a_4 + \gamma_1$, $b = b_4 + \gamma_2$, where γ_1 and γ_2 are small perturbation parameters. Under these assumptions, (8) transforms into the following map:

$$\begin{pmatrix} u \\ v \end{pmatrix} \to \begin{pmatrix} j_{10}(\gamma) & j_{01}(\gamma) \\ k_{10}(\gamma) & k_{01}(\gamma) \end{pmatrix} \begin{pmatrix} u \\ v \end{pmatrix} + \begin{pmatrix} h_1(u, v, \gamma) \\ h_2(u, v, \gamma) \end{pmatrix}, \tag{27}$$

where $\gamma = (\gamma_1, \gamma_2)$

$$\begin{cases} j_{10}(\gamma) = h\left(3 - \dfrac{200}{(a_4 + \gamma_1)^2 + 25}\right) + 1, \\ j_{01}(\gamma) = -\dfrac{20h\,(a_4 + \gamma_1)}{(a_4 + \gamma_1)^2 + 25}, \\ k_{10}(\gamma) = \dfrac{2h\,(a_4 + \gamma_1)^2\,(b_4 + \gamma_2)}{(a_4 + \gamma_1)^2 + 25}, \\ k_{01}(\gamma) = 1 - \dfrac{5h\,(a_4 + \gamma_1)(b_4 + \gamma_2)}{(a_4 + \gamma_1)^2 + 25}. \end{cases}$$

$$\begin{cases} h_1(u, v, \gamma) = j_{20}(\gamma)u^2 + j_{11}(\gamma)uv + O\left((|u| + |v|)^3\right), \\ h_2(u, v, \gamma) = k_{20}(\gamma)u^2 + k_{11}(\gamma)uv + O\left((|u| + |v|)^3\right), \end{cases}$$

$$j_{20}(\gamma) = -\frac{20h\,(a_4+\gamma_1)\left((a_4+\gamma_1)^{\,2}-75\right)}{((a_4+\gamma_1)^{\,2}+25)^{\,2}},$$

$$j_{11}(\gamma) = \frac{100h\,(a_4+\gamma_1-5)\,(a_4+\gamma_1+5)}{((a_4+\gamma_1)^{\,2}+25)^{\,2}},$$

$$k_{20}(\gamma) = -\frac{5h\,(a_4+\gamma_1)\left((a_4+\gamma_1)^{\,2}-75\right)(b_4+\gamma_2)}{((a_4+\gamma_1)^{\,2}+25)^{\,2}},$$

$$j_{11}(\gamma) = \frac{25h\,(a_4+\gamma_1-5)\,(a_4+\gamma_1+5)\,(b_4+\gamma_2)}{((a_4+\gamma_1)^{\,2}+25)^{\,2}}.$$

The characteristic equation of the Jacobian matrix $\begin{pmatrix} j_{10}(\gamma) & j_{01}(\gamma) \\ k_{10}(\gamma) & k_{01}(\gamma) \end{pmatrix}$ for system (27) at $\gamma_1 = \gamma_2 = 0$ yields eigenvalues of the form $\pm i$. Let q and p represent the eigenvectors corresponding to the Jacobian matrix of (27) and its transpose at $\gamma_1 = \gamma_2 = 0$, respectively, with the condition that their inner product satisfies $\langle p, q\rangle = 1$. Through direct calculation, we derive the following:

$$q = \begin{pmatrix} \left(\frac{1}{4}(2-5h) + \frac{1}{4}i(5h)\right)\mu \\ 1 \end{pmatrix},$$

and

$$p = \begin{pmatrix} \frac{2i}{5h\mu} \\ \frac{5h+i(5h-2)}{10h} \end{pmatrix},$$

where

$$\mu := \sqrt{\frac{5h(3h+2)-2}{5h(5h-2)+2}}.$$

Then, every $Y \in \mathbb{R}^2$ can be expressed uniquely in the following manner:

$$Y = zq + \bar{z}\bar{q}, \quad z \in \mathbb{C}.$$

Thus, the complex representation of the map (27) can be expressed as follows:

$$z \longrightarrow iz + \sum_{2\le j+k\le 3} \frac{1}{j!k!} H_{jk}(\gamma) z^j \bar{z}^k, \tag{28}$$

where

$$
\begin{aligned}
H_{20}(\gamma) = & \frac{\left(\frac{1}{5}+\frac{i}{5}\right) j_{11}(\gamma)(5h-1-i)}{h} \\
& - \frac{(5h-1-i)\,\mu}{10h}\Big((5h-1-i)\, j_{20}(\gamma) \\
& + (1+i-5hi)\, k_{11}(\gamma)\Big) \\
& + \frac{\left(\frac{1}{40}+\frac{i}{40}\right) k_{20}(\gamma)(5h-(1+i))^2(5h+(-1+i))\mu^2}{h},
\end{aligned}
$$

$$
\begin{aligned}
H_{11}(\gamma) = & \frac{(1-i)}{20h}\,(5h-1+i)\,\mu\Big((5h-2)\, k_{11}(\gamma) \\
& + + \frac{1-i}{40h}\, k_{20}(\gamma)\,(5h-1-i)(5h-1+i)^2\,\mu^2 \\
& + (2-5h+5ih)\, j_{20}(\gamma)\Big) \\
& + \frac{i(5h-2)}{5h}\, j_{11}(\gamma),
\end{aligned}
$$

$$
\begin{aligned}
H_{02}(\gamma) = & -\frac{\left(\frac{1}{5}-\frac{i}{5}\right) j_{11}(\gamma)(5h+(-1+i))}{h} \\
& + \frac{(5h+(-1+i))^2\mu(j_{20}(\gamma)-k_{11}(\gamma))}{10h} \\
& + \frac{\left(\frac{1}{40}+\frac{i}{40}\right) k_{20}(\gamma)(5h+(-1+i))^3\mu^2}{h},
\end{aligned}
$$

and $H_{30}(\gamma) = H_{21}(\gamma) = H_{12}(\gamma) = H_{03}(\gamma) = 0$.

Following Lemma 9.14 [15, p. 455], it is then possible to construct a smoothly parameterized transformation of variables that facilitates the conversion of the map (28) into the form given below:

$$
\Lambda \to i\Lambda + L(\gamma)\Lambda|\Lambda|^2 + M(\gamma)\bar{\Lambda}^3 + O\left(|\Lambda|^4\right), \tag{29}
$$

where at $\gamma_1 = \gamma_2 = 0$, that is, $\gamma = (0,0)$, $L(0,0)$ and $M(0,0)$ are given as

follows:

$$L(0,0) = \left(\frac{1+3i}{4}\right) H_{20}(0,0)H_{11}(0,0) + \left(\frac{1-i}{2}\right) |H_{11}(0,0)|^2 - \left(\frac{1+i}{4}\right) |H_{02}(0,0)|^2 + \frac{1}{2}H_{21}(0,0),$$

and

$$M(0,0) = \left(\frac{i-1}{4}\right) H_{11}(0,0)H_{02}(0,0) - \left(\frac{i+1}{4}\right) H_{02}(0,0)\bar{H}_{20}(0,0) + \frac{1}{6}H_{03}(0,0).$$

Theorem 3. *Let the parameters be set to their critical values $a = a_4$ and $b = b_4$. The system (8) then undergoes a 1:4 strong resonance at its positive fixed point. Assuming the non-degeneracy conditions $Re(L(0,0)) \neq 0$ and $M(0,0) \neq 0$ for the normal form coefficients of map (29) are satisfied, the system exhibits the following dynamical behaviors in a neighborhood of the bifurcation:*

(i) The system undergoes a Neimark-Sacker bifurcation, leading to the emergence of a unique closed invariant curve. The stability of this curve is determined by the sign of $Re(L(0,0))$.

If $Re(L(0,0)) < 0$, the bifurcation is supercritical, and the invariant curve is stable (attracting).

If $Re(L(0,0)) > 0$, the bifurcation is subcritical, and the invariant curve is unstable (repelling).

(ii) In the vicinity of the fixed point, a pair of period-four orbits is created. One of these orbits is a saddle cycle.

(iii) When the coefficient $M(0,0) \neq 0$, the stable and unstable manifolds of the period-four saddle cycle may intersect. This can create a homoclinic structure, leading to complex dynamics, including the potential for chaotic behavior in certain parameter regions.

3 Numerical simulation

In this section, we seek to validate the theoretical analysis presented earlier by demonstrating the dynamic and chaotic behavior of the system described by

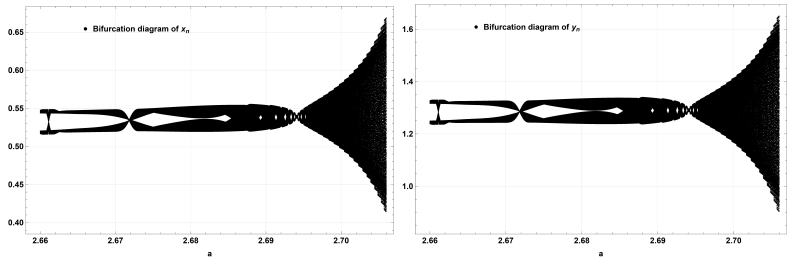

(a) Bifurcation diagram for x_n. **(b)** Bifurcation diagram for y_n.

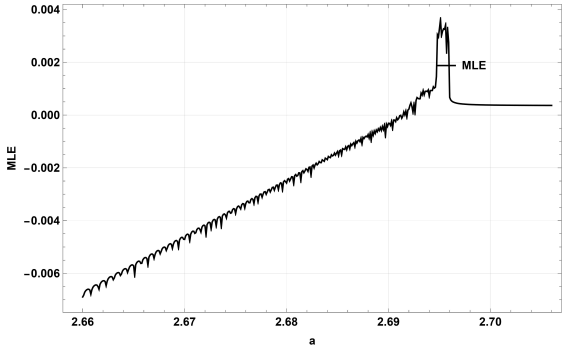

(c) Maximum Lyapunov exponents.

Figure 2. Plots of the system (8) at $h = 0.25$, $b = b_2 = 30.6526$, $(x_0, y_0) = (0.538816, 1.29032)$ and $2.66 \leq a \leq 2.706$.

equation (8). For this, first we discuss emergence of 1:2 strong resonance and bifurcating properties related to this. We choose $h = 0.25$, then 1:2 strong resonance occurs at $a = a_2 = 2.69408$ and $b = b_2 = 30.6526$. Moreover, at $a = a_2 = 2.69408, b = b_2 = 30.6526, h = 0.25$, the fixed point of system (8) is $(0.538816, 1.29032)$, and taking into account the conditions of Theorem 1, one can see that $A(O) = -0.086027$, $B(O) = 0.324687$ and $B(O) + A(O) = 0.0666058$ (that is, conditions of Theorem 1 are satisfied). Furthermore, at $h = 0.25$, $b = b_2 = 30.6526$, $(x_0, y_0) = (0.538816, 1.29032)$ and $2.66 \leq a \leq 2.706$, the bifurcation diagrams and MLE are depicted

in Fig. 2. Moreover, it must be noted that the 1:2 strong resonance is strongly dependent on the step size h. One can check this occurrence between $0.176607 < h < 0.4$. Next, we take $h = 0.18$, then 1:2 strong resonance occurs at $a = a_2 = 18.7548$ and $b = b_2 = 99.1992$. Moreover, at $a = a_2 = 18.7548, b = b_2 = 99.1992, h = 0.18$, the fixed point of system (8) is $(3.75097, 15.0698)$, and taking into account the conditions of Theorem 1, one can see that $A(O) = -0.00107762$, $B(O) = 0.00313415$ and $B(O) + 3A(O) = -0.0000987133$ (that is, conditions of Theorem 1 are satisfied). Furthermore, at $h = 0.18$, $b = b_2 = 99.1992$, $(x_0, y_0) = (3.75097, 15.0698)$ and $18.3 \leq a \leq 20$, the bifurcation diagrams and MLE are depicted in Fig. 3.

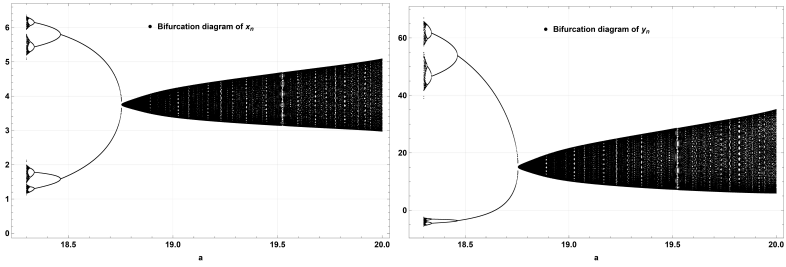

(a) Bifurcation diagram for x_n. **(b)** Bifurcation diagram for y_n.

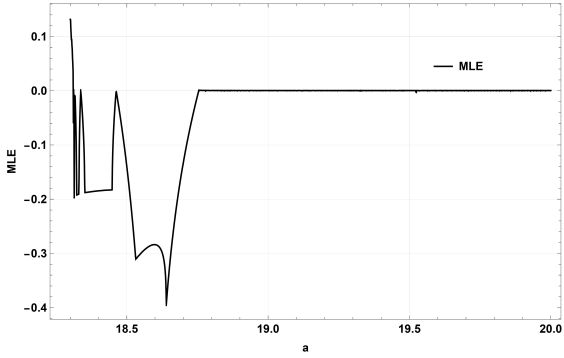

(c) Maximum Lyapunov exponents.

Figure 3. Plots of the system (8) at $h = 0.18$, $b = b_2 = 99.1992$, $(x_0, y_0) = (3.75097, 15.0698)$ and $18.3 \leq a \leq 20$.

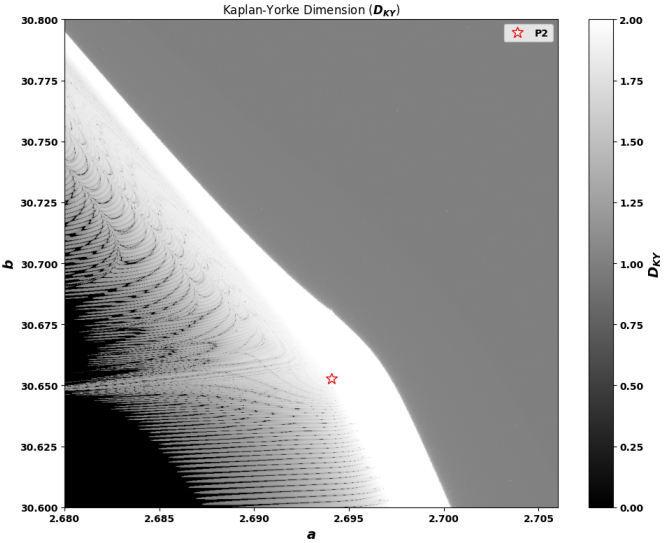

Figure 4. Kaplan-Yorke dimension at $h = 0.25$, $30.68 \leq b \leq 30.8$, $(x_0, y_0) = (0.538816, 1.29032)$ and $2.66 \leq a \leq 2.706$.

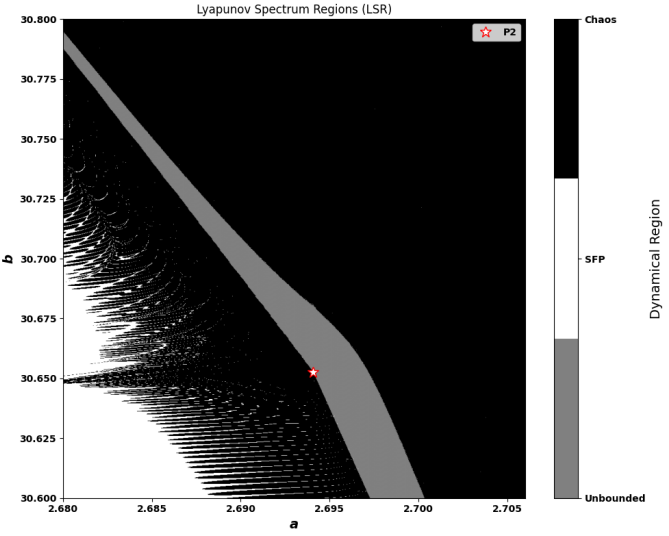

Figure 5. Lyapunov spectrum regions at $h = 0.25$, $30.68 \leq b \leq 30.8$, $(x_0, y_0) = (0.538816, 1.29032)$ and $2.66 \leq a \leq 2.706$.

Moreover, at $h = 0.25$, $(x_0, y_0) = (0.538816, 1.29032)$, $2.66 \leq a \leq 2.706$, and $30.68 \leq b \leq 30.8$, the Kaplan-Yorke dimension (D_{KY}) and the Lyapunov spectrum regions (LSR) are depicted in Fig. 4 and 5, respectively, near 1:2 strong resonance point $P2 = (2.69408, 30.6526)$. Next, we take $h = 0.176$, then system (8) undergoes 1:3 strong resonance at its fixed point $(3.29256, 11.841)$ about resonance point $P3 = (a_3, b_3) = (16.4628, 69.6593)$. Then, it is easy to see that at $h = 0.176$, $P(O) = 1.44951 + 0.488397i$ and $Q(O) = -1.08394 + 2.16944i$, which automatically satisfies the conditions of Theorem 2. Taking $h = 0.176$, $b = b_3 = 69.6593$, and $15.8 \leq a \leq 16.5$, the bifurcation diagram is displayed in Fig. 6. On the other hand, at $h = 0.176$, $a = a_3 = 16.4628$, and $67 \leq b \leq 70$, the bifurcation diagram is displayed in Fig. 7.

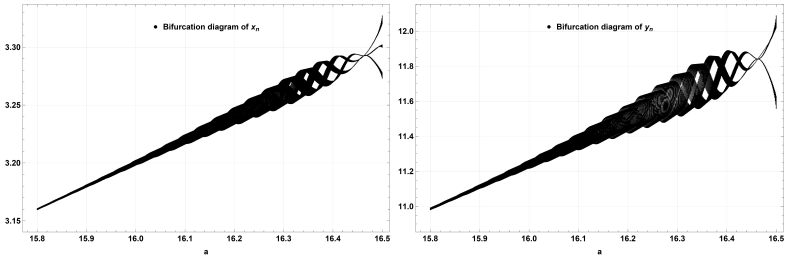

(a) Bifurcation diagram for x_n. **(b)** Bifurcation diagram for y_n.

Figure 6. Bifurcation diagrams of (8) at $h = 0.176$, $b = b_3 = 69.6593$, and $15.8 \leq a \leq 16.5$.

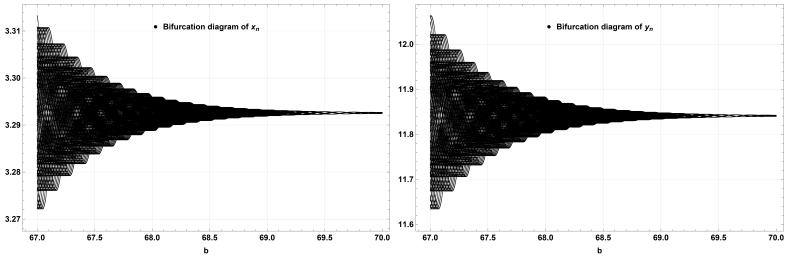

(a) Bifurcation diagram for x_n. **(b)** Bifurcation diagram for y_n.

Figure 7. Bifurcation diagrams of (8) at $h = 0.176$, $a = a_3 = 16.4628$, and $67 \leq b \leq 70$.

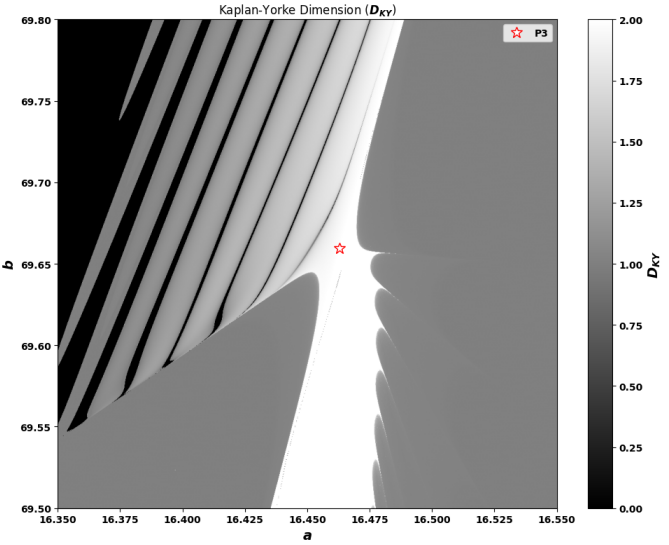

Figure 8. Kaplan-Yorke dimension at $h = 0.176$, $(x_0, y_0) = (3.29256, 11.841)$, $16.35 \leq a \leq 16.55$, and $69.5 \leq b \leq 69.8$.

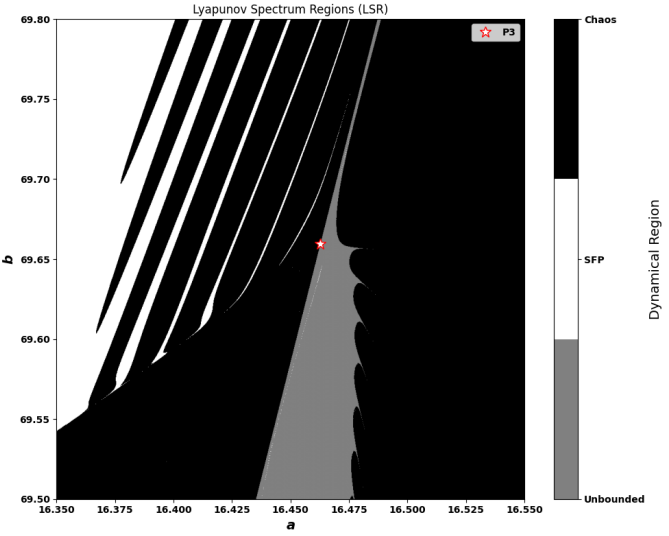

Figure 9. Lyapunov spectrum regions at $h = 0.176$, $(x_0, y_0) = (3.29256, 11.841)$, $16.35 \leq a \leq 16.55$, and $69.5 \leq b \leq 69.8$.

Moreover, at $h = 0.176$, $(x_0, y_0) = (3.29256, 11.841)$, $16.35 \leq a \leq 16.55$, and $69.5 \leq b \leq 69.8$ the Kaplan-Yorke dimension (D_{KY}) and the Lyapunov spectrum regions (LSR) are depicted in Fig. 8 and 9, respectively, near 1:3 strong resonance point $P3 = (16.4628, 69.6593)$. In the end, we check the appearance of 1:4 strong resonance, we take $h = 0.2$, then $a_4 = 6.45497$ and $b_4 = 20.6559$, then system undergoes 1:4 strong resonance at fixed point $(1.29099, 2.66667)$. Moreover, taking $h = 0.2$, $b = b_4 = 20.6559$, $5.5 \leq a \leq 8$, the bifurcation diagrams and MLE are shown in Fig. 10. On the other hand, considering Theorem 3, we have $L(O) = -0.00984375 - 0.00421875i$, and $M(O) = 0.00140625 + 0.0182813i$, clearly verifying its assumptions.

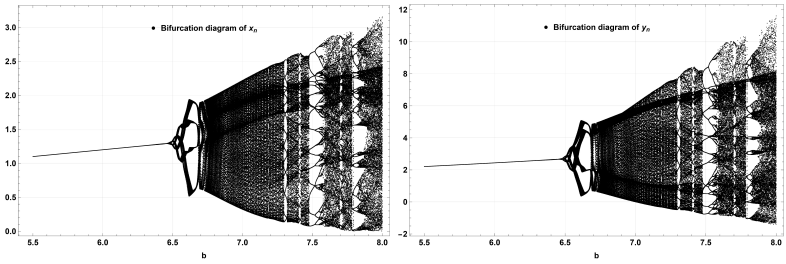

(a) Bifurcation diagram for x_n. **(b)** Bifurcation diagram for y_n.

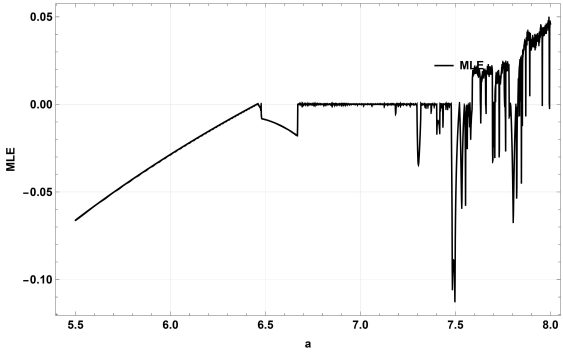

(c) Maximum Lyapunov exponents.

Figure 10. Bifurcation diagrams and MLE of the system (8) at $h = 0.2$, $b = b_4 = 20.6559$, $5.5 \leq a \leq 8$.

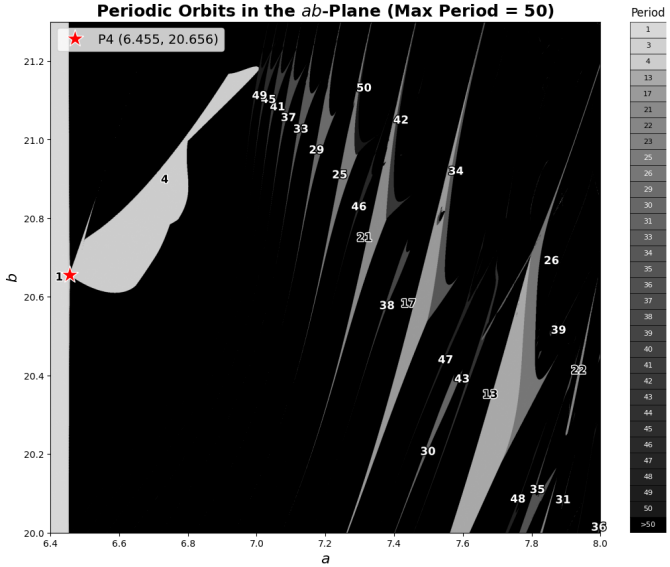

Figure 11. Periodicity diagram near $P4$ point at $h = 0.2$, $6.4 \leq a \leq 8$ and $20 \leq b \leq 21.3$.

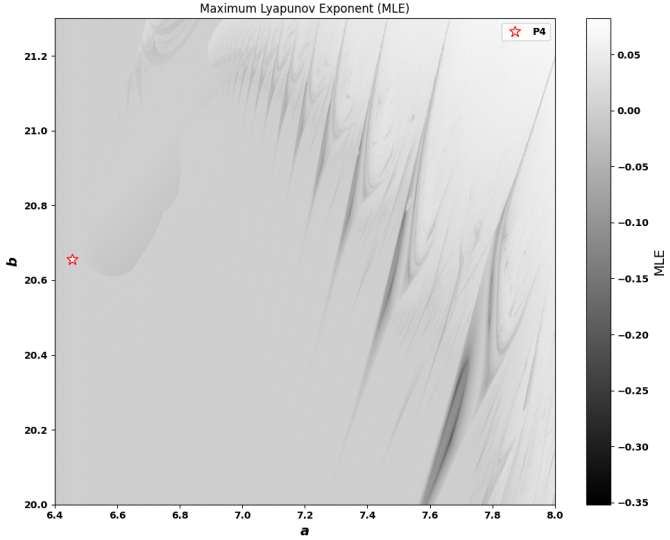

Figure 12. MLE at $h = 0.2$, $(x_0, y_0) = (1.29099, 2.66667)$, $6.4 \leq a \leq 8$, and $20.0 \leq b \leq 21.3$.

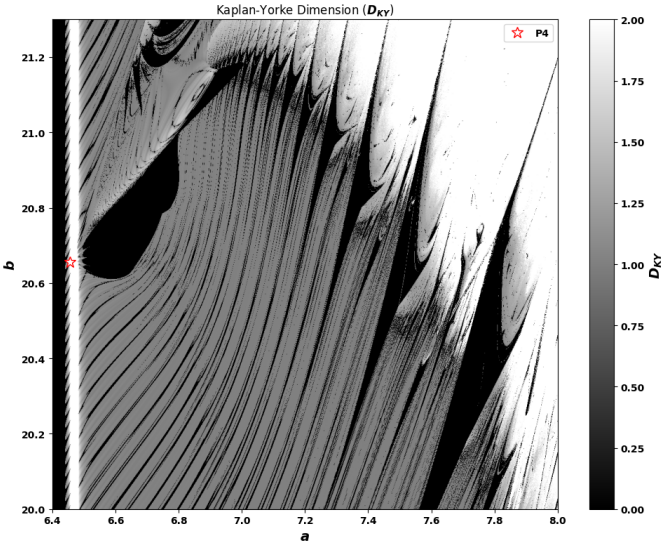

Figure 13. Kaplan-Yorke dimension at $h = 0.2$, $(x_0, y_0) = (1.29099, 2.66667)$, $6.4 \leq a \leq 8$, and $20.0 \leq b \leq 21.3$.

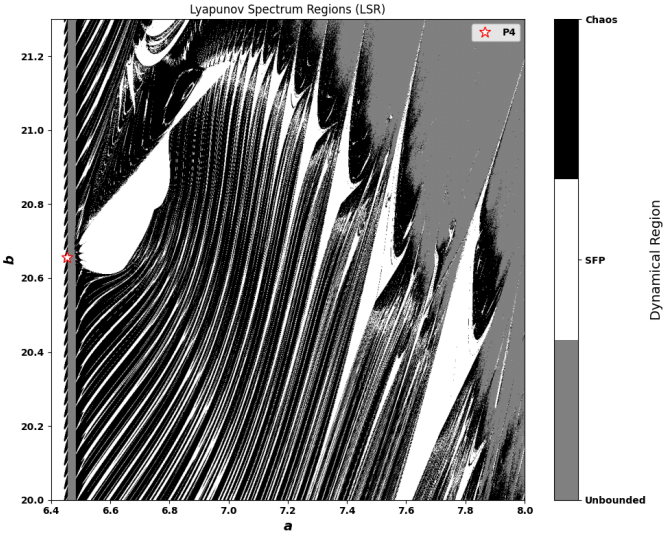

Figure 14. Lyapunov spectrum regions at $h = 0.2$, $(x_0, y_0) = (1.29099, 2.66667)$, $6.4 \leq a \leq 8$, and $20.0 \leq b \leq 21.3$.

Moreover, for $h = 0.2$, $6.4 \leq a \leq 8$ and $20 \leq b \leq 21.3$, the periodic orbits diagram up to 50 periods about 1:4 strong resonance point $P4 = (6.45497,\ 20.6559)$ is depicted in Fig. 11. Moreover, at $h = 0.2$, $(x_0, y_0) = (1.29099, 2.66667)$, $6.4 \leq a \leq 8$, and $20.0 \leq b \leq 21.3$, MLE, Kaplan-Yorke dimension (D_{KY}) and the Lyapunov spectrum regions (LSR) are depicted in Fig. 12, 13, and 14, respectively, near 1:4 strong resonance point $P4 = (6.45497,\ 20.6559)$.

Conclusion

This research provides a definitive investigation into the complex nonlinear dynamics of the discrete-time Chlorine Dioxide-Iodine-Malonic Acid (CDIMA) reaction model, establishing a robust link between analytical theory and numerical validation. By focusing on the unique positive fixed point of the system, $(x^*, y^*) = (\frac{a}{5}, 1 + \frac{a^2}{25})$, we have successfully characterized the codimension–two bifurcations corresponding to 1:2, 1:3, and 1:4 strong resonances. The agreement between the theoretical conditions outlined in Theorems 1, 2, and 3 and the simulated behaviors depicted in Figures 1–14 confirms the rich dynamical repertoire and the predictive power of our approach.

The analysis reveals three distinct dynamical regimes, each governed by a specific strong resonance:

- **1:2 Strong Resonance:** The conditions for this resonance, governed by Theorem 1, were shown to initiate a period-doubling bifurcation leading to stable period-2 limit cycles. This chemically represents a rhythmic, bistable oscillation. Our numerical simulations for $h = 0.25$ at the critical point $(a_2, b_2) \approx (2.69, 30.65)$ confirmed this, satisfying the condition $B(O) + 3A(O) > 0$ of theorem. Figure 2 provides a clear visual of this transition, while the parameter–plane plots in Figures 4 and 5 map the regions of stability and chaos around the bifurcation point P_2, vividly illustrating the complex dynamics predicted by the theorem. The robustness of this finding is further supported by the analysis at $h = 0.18$ (Figure 3), which demonstrates the same phenomena under different parameters.

- **1:3 Strong Resonance:** The emergence of complex period-3 orbits, indicative of tripled-state nonlinear interactions, was analyzed through Theorem 2. The non-degeneracy conditions $P(O) \neq 0$ and $\mathrm{Re}(Q(O)) \neq 0$ were verified for $h = 0.176$ at $(a_3, b_3) \approx (16.46, 69.66)$, ensuring the creation of period-three orbits and the potential for homoclinic structures leading to chaos. The bifurcation diagrams in Figure 6 (varying a) and Figure 7 (varying b) numerically realize these predictions, showing the evolution of the system into intricate patterns. Furthermore, the Kaplan–Yorke dimension and Lyapunov spectrum regions in Figures 8 and 9 provide a detailed map of the parameter space near the P_3 point, confirming the presence of chaotic regions arising from the interactions predicted in Theorem 2.

- **1:4 Strong Resonance:** This resonance introduces a mixed regime of periodic and chaotic dynamics, characterized by a sensitive dependence on initial conditions. The dynamics are governed by Theorem 3, whose conditions $\mathrm{Re}(L(0,0)) < 0$ and $M(0,0) \neq 0$ were met for $h = 0.2$ at $(a_4, b_4) \approx (6.45, 20.66)$. This guarantees the emergence of a stable invariant curve and period-four orbits, alongside homoclinic intersections that generate chaos. Figure 10 illustrates this path to chaos, while the periodicity diagram in Figure 11 offers compelling evidence by visualizing the large period–4 orbit region emanating from the P_4 point, surrounded by a sea of chaos dotted with periodic windows. The comprehensive mapping in Figures 12–14 further substantiates these findings, illustrating the rich fractal structures of the periodic and chaotic regions in the parameter plane.

In summary, this work provides a comprehensive validation of the theoretical framework for codimension-two bifurcations in the CDIMA model. The remarkable consistency between our analytical theorems and extensive numerical simulations advances the fundamental understanding of how complex oscillatory patterns and chaos arise in nonlinear chemical systems. These insights hold practical implications for controlling reaction dynamics, offering a predictive basis to stabilize oscillations or mitigate chaos in engineered and biological systems. The integrated methodology estab-

lished here serves as a powerful and generalizable approach for exploring complex behaviors in other nonlinear systems.

***Acknowledgment*:** The authors extend their appreciation to the Deanship of Scientific Research at Northern Border University, Arar, KSA, for funding this research work through the project number NBU-FFR-2025-2230-11

References

[1] I. Lengyel, G. Ribai, I. R. Epstein, Experimental and modeling study of oscillations in the chlorine dioxide–iodine–malonic acid reaction, *J. Am. Chem. Soc.* **112** (1990) 9104–9110.

[2] L. Cyorgyi, R. J. Field, Simple models of deterministic chaos in the Belousov– Zhabotinsky reaction, *J. Phys. Chem.* **95** (1991) 6594–6602.

[3] B. Swathi, V. R. Kulkarni, Simulation of few bifurcation phase diagrams of Belousov–Zhabotinsky reaction with eleven variable chaotic model in CSTR, *J. Chem.* **6** (2009) 481–488.

[4] E. Mosekilde, *Topics in Nonlinear Dynamics: Applications to Physics, Biology and Economic Systems*, World Scientific, New Jersey, 1996.

[5] Q. Din, T. Donchev, D. Kolev, Stability, bifurcation analysis and chaos control in chlorine dioxide–iodine–malonic acid reaction, *MATCH Commun. Math. Comput. Chem.* **79** (2018) 577–606.

[6] D. Mu, C. Xu, Z. Liu, Y. Pang, Further insight into bifurcation and hybrid control tactics of a chlorine dioxide–iodine–malonic acid chemical reaction model incorporating delays, *MATCH Commun. Math. Comput. Chem.* **89** (2023) 529–566.

[7] M. S. Khan, Bifurcation analysis of a discrete–time four–dimensional cubic autocatalator chemical reaction model with coupling through uncatalysed reactant, *MATCH Commun. Math. Comput. Chem.* **87** (2022) 415–439.

[8] M. S. Khan, M. Ozair, T. Hussain, J. F. Gómez, Bifurcation analysis of a discrete–time compartmental model for hypertensive or diabetic patients exposed to COVID–19, *Eur. Phys. J. Plus.* **136** (2021) 1–26.

[9] M. A. Abbasi, O. Albalawi, R. Niaz, Modeling and dynamical analysis of an ecological population with the Allee effect, *Int. J. Dyn. Contr.* **12** (2024) 1–27.

[10] M. A. Abbasi, M. Samreen, Analyzing multi-parameter bifurcation on a prey?predator model with the Allee effect and fear effect, *Chaos. Soliton. Fract.* **180** (2024) #114498.

[11] Q. Din, M. S. Shabbir, M. A. Khan, A cubic autocatalator chemical reaction model with limit cycle analysis and consistency preserving discretization, *MATCH Commun. Math. Comput. Chem.* **87** (2022) 441–462.

[12] M. A. Khan, Q. Din, Codimension-one and codimension-two bifurcations of a fractional-order cubic autocatalator chemical reaction system, *MATCH Commun. Math. Comput. Chem.* **91** (2024) 415–452.

[13] E. E. Selkov, Self-oscillations in glycolysis. A simple model, *Eur. J. Biochem.* **4** (1968) 79–86.

[14] B. P. Belousov, An oscillating reaction and its mechanism, *Sborn. Referat. Radiat. Med. Medgiz.*, 1959, pp. 145–145.

[15] Y. A. Kuznetsov, *Elements of Applied Bifurcation Theory,* Springer, New York, 2004.

[16] F. A. Davidson, B. P. Rynne, Apriori bounds and global existence of solutions of the steady-state Sel'kov model, *Proc. R. Soc. Edinb. Sect. A.* **130** (2000) 507–516.

[17] M. X. Wang, Non-constant positive steady-states of the Sel'kov model, *J. Diff. Eq.* **190** (2003) 600–620.

[18] R. Peng, Qualitative analysis of steady states to the Sel'kov model, *J. Diff. Eq.* **241** (2007) 386–398.

[19] M. Wei, J. Wu, G. Guo, Steady state bifurcations for a glycolysis model in biochemical reaction, *Nonlin. Anal. RWA*. **22** (2015) 155–175.

[20] J. D. Murray, *Mathematical Biology II – Spatial Models and Biomedical Applications*, Springer, New York, 2001.

[21] A. M. Zhabotinskii, Periodic process of the oxidation of malonic acid in solution (Study of the kinetics of Belousov's), *Biofzika* **9** (1964) 306–311.

[22] J. D. Murray, *Mathematical Biology*, Springer, Heidelberg, 1993.

[23] D. S. Jones, M. J. Plank, B. D. Sleeman, *Differential Equations and Mathematical Biology*, CRC Press, Boca Raton, 2009.

[24] R. P. Agarwal, P. J. Y. Wong, *Advance Topics in Difference Equations*, Kluwer, Dordrecht, 1997.

[25] R. Kapral, Discrete models for chemically reacting systems, *J. Math. Chem.* **6** (1991) 113–163.

[26] R. K. Pearson, *Discrete-Time Dynamic Models*, Oxford University Press, Oxford, 1999.

[27] C. A. Floudas, X. Lin, Continuous-time versus discrete-time approaches for scheduling of chemical processes: a review, *Comput. Chem. Eng.* **28**(2004) 2109–2129.

[28] S. H. Strogatz, *Nonlinear Dynamics and Chaos with Applications to Physics, Biology, Chemistry and Engineering*, Addison-Wesley, New York, 1994.

[29] M. Chen, R. Wu, Dynamics of a harvested predator-prey model with predator-taxis, *Bull. Malays. Math. Sci. Soc.* **46**(2023).

[30] M. Chen, Z. Hu, Q. Zheng, H. M. Srivastava, Dynamics analysis of a spatiotemporal SI model, *Alexandria Eng. J.* **74** (2023)705–714.

[31] M. Chen, J. Kim, S. Ham, Patterns of a general chemical model involving Degn-Harrison reaction scheme, *MATCH Commun. Math. Comput. Chem.* **93** (2025) 267–290.

[32] M. Chen, Hopf bifurcation and self-organization pattern of a modified Brusselator model, *MATCH Commun. Math. Comput. Chem.* **90** (2023) 581–607.

[33] M. Chen, J. Kim, S. Ham, Patterns of a general chemical model involving Degn-Harrison reaction scheme, *MATCH Commun. Math. Comput. Chem.* **93** (2025) 267–290.

[34] M. Chen, X. Z. Li, Stability analysis and Turing pattern of an enzyme-catalyzed reaction model, *MATCH Commun. Math. Comput. Chem.* **94** (2025).